Coupled Systems Mechanics, *Vol. 4, No. 4 (2015) 337-364*
DOI: http://dx.doi.org/10.12989/csm.2015.4.4.337

Plasticity-damage model parameters identification for structural connections

Ismar Imamovic*[1,2], Adnan Ibrahimbegovic[1], Catherine Knopf-Lenoir[1] and Esad Mesic[2]

[1]*Laboratoire Roberval, Université de Technologie de Compiègne / Sorbonne Universités, France*
[2]*Faculty of Civil Engineering, University Sarajevo, Sarajevo, Bosnia and Herzegovina*

(Received January 9, 2015, Revised December 20, 2015, Accepted December 21, 2015)

Abstract. In this paper we present methodology for parameters identification of constitutive model which is able to present behavior of a connection between two members in a structure. Such a constitutive model for frame connections can be cast in the most general form of the Timoshenko beam, which can present three failure modes. The first failure mode pertains to the bending in connection, which is defined as coupled plasticity-damage model with nonlinear softening. The second failure mode is seeking to capture the shearing of connection, which is defined as plasticity with linear hardening and nonlinear softening. The third failure mode pertains to the diffuse failure in the members; excluding it leads to linear elastic constitutive law. Theoretical formulation of this Timoshenko beam model and its finite element implementation are presented in the second section. The parameter identification procedure that will allow us to define eighteen unknown parameters is given in Section 3. The proposed methodology splits identification in three phases, with all details presented in Section 4 through three different examples. We also present the real experimental results. The conclusions are stated in the last section of the paper.

Keywords: identification; connection; coupled plasticity-damage; Euler-Bernoulli and Timoshenko beam

1. Introduction

In this paper we present methodology for identification parameters of model which is able to present behavior of a connection between two members in a structure. These connections have very important effect upon nonlinear behavior of frame structures, especially, those built of steel and timber. Many types of connection all of exist and practically each of them has something specific. Thus, the best choice of adequate model for describing these phenomena is very challenging task.

The Timoshenko beam (e.g., Medic *et al*. 2013) provides the possibility for constructing the optimal model of this kind. There precisely, we use coupled plasticity-damage model (e.g., Ibrahimbegovic *et al*. 2008, Ayhan *et al*. 2013) with includes softening response (e.g., Ibrahimbegovic 2009). Plasticity and damage models are defined with linear hardening, while softening response is defined with nonlinear law. Transverse displacement or shearing of the

*Corresponding author, Ph.D. Student, E-mail: imamovic.ismar@gmail.com

http://www.techno-press.org/?journal=csm&subpage=7 ISSN: 2234-2184 (Print), 2234-2192 (Online)

connection is defined with plasticity model with softening. Theoretical formulation of the joint element which can describe this kind of behavior for bending and shearing is presented in the next section of the paper.

Each member of frame structure is modeled with the Euler-Bernoulli beam (e.g., Dujc *et al*. 2010). Constitutive law is defined as plasticity with linear hardening and nonlinear softening models. This type of beam model is adequate for slender elements where length *l* of the elements versus high *h* ratio l/h >10. We note in passing that, although the temperature effects in steel structures can very important (e.g., Ibrahimbegovic *et al*. 2013), in this work such an effect is completely neglected. Rather, the main focus of this research pertains to identification of model parameters for the connection between two members of a structure.

The identification of model parameters can be split into three subsequent phases, in following (Kucherova *et al*. 2009). In the first phase we present identification of parameters governing the elasticity response, where we have three unknowns. The second phase deals with identification of parameters for coupled plasticity-damage model. Two unknown parameters are active in Euler-Bernoulli beam and six parameters in the connection. Identification of connection behavior can be split into the shearing and the bending. In the bending case there are two possible scenarios, first when parameters for plasticity and damage models take very close values, and the second when the values of parameters are not as close, so that we can identify two by two parameters.

The identification of these parameters in each phase is done using combination of two software programs Matlab (The MathWorks, Inc., Natick, Massachusetts, United States) and FEAP (e.g., Zienkiewicz and Taylor 2005). FEAP is the finite element program which is used for FEM analysis task in the identification process. Matlab is used for computing the minimization of objective or cost function. Objective functions for different phases of identification are presented in the third section of this paper.

The outline of the paper is as follows. In the next section we present the main ingredients of the proposed joint element for the presenting behavior of connection in terms of the Timoshenko beam (e.g., Bui *et al*. 2014). In the third section we describe the global identification problem of connection. The fourth section presents proposition for experimental setup, loading program and all phases of identification in three different examples. In the fifth section we also compare examples of identification against real experimental results (e.g., Gang Shi *et al*. 2007, Mesic 2003).

2. Theoretical formulation of the Timoshenko beam audits finite element implementation

In this section we present theoretical formulations for the joint element in terms of the Timoshenko beam. The joint element is slight modification of the Timoshenko beam defined in (Bui *et al*. 2014, Nikolic and Ibrahimbegovic 2015) with embedded discontinuity. The need for this modification can be found in physically admissible displacement/deformation of connections. Namely, for pure bending in the connection there does not exist transverse displacement and if we use Timoshenko or Euler-Bernoulli beam this condition is not satisfied. The modification of the Timoshenko beam starts in Eq. (1), where we modify expression for the shear deformation. The Euler-Bernoulli beam with embedded discontinuity (e.g., Dujc *et al.* 2010) is used to present bending behavior of members of the frame structure. Constitutive law is defined as plasticity with linear hardening for continuous part and discontinuity defining the softening according the

nonlinear law.

2.1 Timoshenko modified beam element

The theoretical formulation of the joint element - modified Timoshenko beam can first be defined in terms of its strong form of equilibrium equation, there we present the main ingredients of these models.

2.1.1 Strong form of equilibrium equations

In Fig. 1 we present different formulation of beam curvature measure in a given cross section. It can be written

$$\begin{aligned} &\frac{dv}{dx} = \theta && \text{- Euler-Bernoulli beam} \\ &\frac{dv}{dx} = \theta + \gamma && \text{- Timoshenko beam} \\ &\frac{dv}{dx} = \gamma && \text{- Joint element - modified T. beam} \end{aligned} \tag{1}$$

where γ is shear deformation of the beam cross section.

Equilibrium equations at the infinitesimal beam

$$\left.\begin{aligned} \Sigma M_{right-side} = M + dM - M - Vdx + \underbrace{q(x)dx\frac{dx}{2}}_{\approx 0 \text{ (small def.)}} = 0 \rightarrow V = \frac{dM}{dx} \\ \Sigma V = V - V - dV - q(x)dx = 0 \rightarrow \frac{dV}{dx} = -q(x) \end{aligned}\right\} \rightarrow \frac{d^2M}{dx^2} = -q(x) \tag{2}$$

Relation between internal forces and deformations when restricted to linear elasticity

$$M(x) = EI\frac{d\theta}{dx}; V(x) = GA_v\left(\frac{dv}{dx} - \theta\right) \text{ - Timoshenko beam} \tag{3}$$

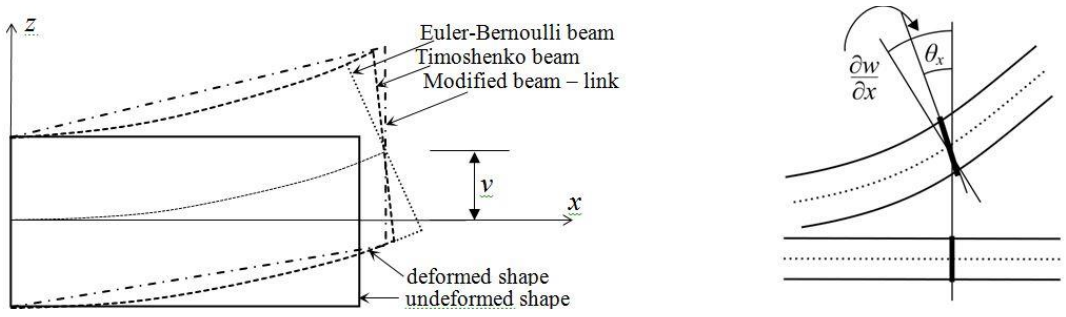

Fig. 1 Deformation of beams

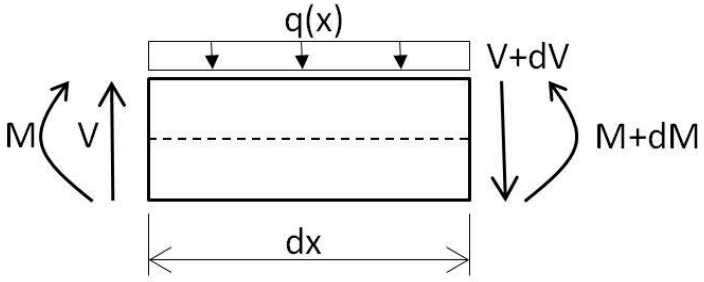

Fig. 2 Equilibrium at the infinitesimal beam

$$M(x) = EI\frac{d\theta}{dx}; V(x) = GA_v\left(\frac{dv}{dx}\right) \text{ - Joint element} \tag{4}$$

Using Eqs. (1)-(3) we can obtain the strong form of the equilibrium equations

$$\text{Timoshenko beam: } \left.\begin{aligned} &\frac{d^2}{dx^2}\left(EI\frac{d\theta}{dx}\right) = -q(x) \\ &\frac{dv}{dx} = \theta - \frac{EI}{GA_v}\frac{d^2\theta}{dx^2} \end{aligned}\right\} \rightarrow EI\frac{d^4v}{dx^4} = q(x) - \frac{EI}{GA_v}\frac{d^2q}{dx^2} \tag{5}$$

$$\text{Joint element: } \left.\begin{aligned} &\frac{d^2}{dx^2}\left(EI\frac{d\theta}{dx}\right) = -q(x) \\ &\frac{dv}{dx} = \frac{EI}{GA_v}\frac{d^2\theta}{dx^2} \end{aligned}\right\} \rightarrow \frac{d^2v}{dx^2}GA_v = -q(x) \tag{6}$$

2.1.2 Weak form of equilibrium equations

The corresponding weak form of equilibrium equation can be written in the standard form for both beams (e.g., Nikolic *et al*. 2014)

$$G(\varepsilon, \zeta^p, \zeta^d; \delta w) = \int_0^l \boldsymbol{\sigma}^T \delta\boldsymbol{\varepsilon} dx - \underbrace{\int_0^l \mathbf{f}^T \delta\mathbf{w} dx - \mathbf{F}^T \delta\mathbf{w}}_{External\ \ force} = 0 \tag{7}$$

where $\boldsymbol{\sigma} = \left[M, T, N\right]^T$ is the stress resultant force, $\delta\boldsymbol{\varepsilon} = \left[\delta\kappa, \delta\gamma, \delta\varepsilon^N\right]$ is a vector of virtual deformations, $\mathbf{f} = \left[m, q, n\right]^T$ is vector of the external distributed load, $\delta\mathbf{w} = \left[\delta\theta, \delta w, \delta u\right]$ is a generalized virtual displacement and $\mathbf{F} = \left[M^{ext}, T^{ext}, N^{ext}\right]^T$ is vector of the external concentrated end forces.

Generalized displacements are split into regular part and jump point introducing the generalized displacement discontinuity

$$\mathbf{u}(x,t)=\bar{\mathbf{u}}(x,t)+\boldsymbol{\alpha}(t)H_{\bar{x}}(x)=\begin{bmatrix}\bar{u}(x,t)\\ \bar{v}(x,t)\\ \bar{\theta}(x,t)\end{bmatrix}+\begin{bmatrix}\alpha_u(t)\\ \alpha_v(t)\\ \alpha_\theta(t)\end{bmatrix}H_{\bar{x}}(x);\;\; H_{\bar{x}}(x)=\begin{cases}1;\;\; x>\bar{x}\\ 0;\; x\le\bar{x}\end{cases} \tag{8}$$

where $\boldsymbol{\alpha}$ is vector of generalized displacement jumps at the point $\bar{x}$, $H_{\bar{x}}(x)$ is the Heaviside function and $\bar{\mathbf{u}}(x,t)$ is vector of regular displacements in the beam.

2.1.3 Constitutive equations for bending

In this section we present constitutive models for bending strains, both the continuous part and the discontinuity. The continuous part is defined with coupled plasticity-damage model, with linear hardening and nonlinear softening. The main ingredients of the coupled plasticity - damage model (e.g., Ibrahimbegovic *et al.* 2007) are

- additive decomposition of the regular curvature field of the beam

$$\bar{\kappa}=\bar{\kappa}^e+\bar{\kappa}^p+\bar{\kappa}^d \tag{9}$$

- Helmholtz free energy

$$\begin{aligned}&\bar{\Psi}\left(\bar{\varepsilon}^e,\bar{\varepsilon}^d,\bar{\xi}^p,\bar{\xi}^d\right)=\underbrace{\frac{1}{2}\bar{\varepsilon}^E\,\bar{\varepsilon}^e}_{\bar{\Psi}^e}+\underbrace{\frac{1}{2}\bar{\xi}^p\bar{K}_p\bar{\xi}^p}_{\bar{\Xi}^p}+\underbrace{\sigma\bar{\varepsilon}^d-\frac{1}{2}\sigma D\sigma}_{\bar{\Psi}^d}+\underbrace{\frac{1}{2}\bar{\xi}^d\bar{K}_d\bar{\xi}^d}_{\bar{\Xi}^d}\\ &\bar{\bar{\Psi}}\left(\bar{\bar{\xi}}^s\right)=\underbrace{\frac{1}{2}\bar{\bar{\xi}}^s\bar{K}_s\bar{\bar{\xi}}^s}_{\bar{\bar{\Xi}}^s};\;\; \Psi(\cdot)=\bar{\Psi}(\cdot)+\bar{\bar{\Psi}}(\bar{\bar{\xi}}^s)\delta_{\bar{x}}\end{aligned} \tag{10}$$

where E is the elasticity modulus, $\bar{\xi}^p,\bar{\xi}^d,\bar{\xi}^s$ are internal hardening variables for: plasticity, damage and softening, respectively, $\boldsymbol{\sigma}=[M]$ is internal force in integration point, $\bar{K}_d,\bar{K}_p$ are hardening moduli for damage and plasticity, and $\bar{K}_s$ is softening modulus.

- the total dissipation produced by this coupled plasticity-damage model, must be remain non-negative. That can be written by appealing to the second principle of thermodynamics

$$0\le\bar{\mathcal{D}}=\underbrace{\dot{\bar{M}}\left(\frac{\partial\bar{\chi}^e}{\partial M}-\bar{\kappa}^e\right)+\dot{M}\left(\frac{\partial\bar{\chi}^d}{\partial M}-\bar{\kappa}^d\right)}_{\bar{\mathcal{D}}^e=0}+\underbrace{M\dot{\bar{\kappa}}^p-\frac{\partial\bar{\bar{\Xi}}^p}{\partial\bar{\xi}^p}\dot{\bar{\xi}}^p}_{\bar{\mathcal{D}}^p}+\underbrace{\frac{\partial\bar{\kappa}^d}{\partial\bar{D}}\dot{\bar{D}}-\frac{\partial\bar{\bar{\Xi}}^d}{\partial\bar{\xi}^d}\dot{\bar{\xi}}^d}_{\bar{\mathcal{D}}^d} \tag{11}$$

where $\bar{\chi}$ is complementary energy, see Ibrahimbegovic (2009).

- yield functions for plasticity and damage

$$\begin{aligned}\bar{\phi}^p\left(M,\bar{q}^p\right)&=|M|-\left(M_y-\bar{q}^p\right)\le 0\\ \bar{\phi}^d\left(M,\bar{q}^d\right)&=|M|-\left(M_f-\bar{q}^d\right)\le 0\end{aligned} \tag{12}$$

where $M_y > 0$ denotes the yield stress, $M_f > 0$ denotes the damage stress at the start of the fracture process zone initiation.

- The principle of maximum plastic dissipation states that among all the variables $\left(M,\bar{q}^{p}\right)$ that satisfy the yield criteria $\bar{\phi}^{p}\left(M,\bar{q}^{p}\right)$. This can be written as a constrained minimization problem

$$\min_{M,\bar{q}^{p}} \max_{\dot{\bar{\gamma}}^{p}} \left[\bar{L}^{p}(M,\bar{q}^{p},\dot{\bar{\gamma}}^{p}) = -\bar{\mathcal{D}}^{p}(M,\bar{q}^{p}) + \dot{\bar{\gamma}}^{p} \cdot \bar{\phi}^{p}(M,\bar{q}^{p}) \right] \tag{13}$$

where the plastic multiplier $\dot{\bar{\gamma}}^{p} \geq 0$ plays the role of Lagrange multiplier. The corresponding Kuhn-Tucker optimality condition, constrained for this minimization problem can provide the evolution equations for internal variables along the loading/unloading conditions

$$\begin{aligned} &\frac{\partial \bar{L}^{p}}{\partial M} = -\dot{\bar{\kappa}}^{p} + \dot{\bar{\gamma}}^{p} \frac{\partial \bar{\phi}}{\partial M} = 0 \Rightarrow \dot{\bar{\kappa}}^{p} = \dot{\bar{\gamma}}^{p} sign(M) \\ &\frac{\partial \bar{L}^{p}}{\partial \bar{q}} = -\dot{\bar{\xi}}^{p} + \dot{\bar{\gamma}}^{p} \frac{\partial \bar{\phi}}{\partial \bar{q}} = 0 \Rightarrow \dot{\bar{\xi}}^{p} = \dot{\bar{\gamma}}^{p} \\ &\dot{\bar{\gamma}}^{p} \geq 0, \;\; \bar{\phi}^{p} \leq 0, \;\; \dot{\bar{\gamma}}^{p} \bar{\phi}^{p} = 0 \end{aligned} \tag{14}$$

The correct value of plasticity multiplier $\dot{\bar{\gamma}}^{p}$ can be computed from the plastic consistency condition

$$0 < \dot{\bar{\gamma}}^{p}; \;\; \bar{\phi}^{p} = 0; \;\; \dot{\bar{\phi}}^{p} = 0 \;\Rightarrow\; \dot{\bar{\gamma}}^{p} = \frac{\dfrac{\partial \bar{\phi}^{p}}{\partial \sigma} E(\dot{\bar{\kappa}} - \dot{\bar{\kappa}}^{d})}{\dfrac{\partial \bar{\phi}^{p}}{\partial M} E \dfrac{\partial \bar{\phi}^{p}}{\partial M} - \dfrac{\partial \bar{\phi}^{p}}{\partial \bar{q}^{p}} \dfrac{\partial \bar{q}^{p}}{\partial \bar{\xi}^{p}} \dfrac{\partial \bar{\phi}^{p}}{\partial \bar{q}^{p}}} \tag{15}$$

The principle of maximum damage dissipation states that among all the variables $(M,\bar{q}^{d})$ that satisfy the yield criteria $\bar{\phi}^{d}\left(M,\bar{q}^{d}\right)$, we have to select those that maximize damage dissipation. This can be written as a constrained minimization problem:

$$\min_{M,\bar{q}^{d}} \max_{\dot{\bar{\gamma}}^{d}} \left[\bar{L}^{d}(M,\bar{q}^{d},\dot{\bar{\gamma}}^{d}) = -\bar{\mathcal{D}}^{d}(M,\bar{q}^{d}) + \dot{\bar{\gamma}}^{d} \cdot \bar{\phi}^{d}(M,\bar{q}^{d}) \right] \tag{16}$$

where the damage multiplier $\dot{\bar{\gamma}}^{d} \geq 0$ plays the role of Lagrange multiplier. By appealing to the Kuhn-Tucker optimality conditions, from the last result we can provide the evolution equations for internal variables along the loading/unloading conditions

$$\begin{aligned} &\frac{\partial \bar{L}^{d}}{\partial M} = -\dot{D}M + \dot{\bar{\gamma}}^{d} \frac{\partial \bar{\phi}^{d}}{\partial M} = 0 \Rightarrow \dot{D} = \dot{\bar{\gamma}}^{d} \frac{1}{M} sign(M) \\ &\frac{\partial \bar{L}^{d}}{\partial \bar{q}^{d}} = -\dot{\bar{\xi}}^{d} + \dot{\bar{\gamma}}^{d} \frac{\partial \bar{\phi}^{d}}{\partial \bar{q}^{d}} = 0 \Rightarrow \dot{\bar{\xi}}^{d} = \dot{\bar{\gamma}}^{d} \end{aligned} \tag{17}$$

The damage consistency conditions can finally provide the correct value for damage multiplier $\dot{\bar{\gamma}}^{d}$

$$\dot{\bar{\gamma}}^{d} \geq 0, \;\; \bar{\phi}^{d} \leq 0, \;\; \dot{\bar{\gamma}}^{d} \bar{\phi}^{d} = 0 \tag{18}$$

$$0<\dot{\bar{\gamma}}^d;\ \ \bar{\phi}^d=0;\ \ \dot{\bar{\phi}}^d=0\ \Rightarrow\ \dot{\bar{\gamma}}^d=\frac{\frac{\partial\bar{\phi}^d}{\partial M}\bar{D}^{-1}\dot{\bar{\kappa}}^d}{\frac{\partial\bar{\phi}^d}{\partial M}\bar{D}^{-1}\frac{\partial\bar{\phi}^d}{\partial M}-\frac{\partial\bar{\phi}^d}{\partial\bar{q}^d}\frac{\partial\bar{q}^d}{\partial\bar{\xi}^d}\frac{\partial\bar{\phi}^d}{\partial\bar{q}^d}} \tag{19}$$

- By enforcing the condition that bending moment has same value in both constitutive models, we can obtain bending moment rate constitutive equation for coupled damage/plasticity model and define the corresponding elasto-plastic-damage tangent modulus

$$\dot{M}=C^{epd}\dot{\bar{\kappa}}=C^{ep}(\dot{\bar{\kappa}}-\dot{\bar{\kappa}}^p-\dot{\bar{\kappa}}^d)=C^{ed}\dot{\bar{\kappa}}^d\Rightarrow C^{epd}=\frac{C^{ep}C^{ed}}{C^{ep}+C^{ed}} \tag{20}$$

The remaining model ingredients define the softening response. In particular we have

- Yield criteria for plasticity in the discontinuity can be written

$$\bar{\bar{\phi}}(t_M,\bar{\bar{q}}^s)=|t_M|-\left(t_{M_u}-\bar{\bar{q}}^s\right)\le 0 \tag{21}$$

where t_M is bending traction, t_{M_y} is ultimate bending traction and $\bar{\bar{q}}^s(\bar{\bar{\xi}}^s)$ is softening stress like variable at the discontinuity.

- The principle of maximum plastic dissipation at discontinuity states that among all admissible variables $(t_M,\bar{q}^s)$ that satisfy the yield criteria $\bar{\bar{\phi}}^s\left(t_M,\bar{\bar{q}}^s\right)$ the ones we choose are those that maximize softening dissipation. This can be written as a constrained minimization problem

$$\min_{t_M,\bar{\bar{q}}^s}\ \max_{\dot{\bar{\bar{\gamma}}}^p}\left[\bar{\bar{L}}^s(t_M,\bar{\bar{q}}^s,\dot{\bar{\bar{\gamma}}}^s)=-\bar{\bar{\mathcal{D}}}^s(t_M,\bar{\bar{q}}^s)+\dot{\bar{\bar{\gamma}}}^s\cdot\bar{\bar{\phi}}^s(t_M,\bar{\bar{q}}^s)\right] \tag{22}$$

where $\dot{\bar{\bar{\gamma}}}^s\ge 0$ plays the role of Lagrange multiplier, $\bar{\bar{\mathcal{D}}}^s=\bar{\bar{q}}^s\dot{\bar{\bar{\xi}}}^s$ is dissipation of the energy in the softening process . By using Kuhn-Tucker loading/unloading condition, the last result can provide the evolution equations for softening internal variables

$$\begin{aligned}
&\frac{\partial\bar{\bar{L}}^s}{\partial t_M}=-\dot{\alpha}_\theta+\dot{\bar{\bar{\gamma}}}^s\frac{\partial\bar{\bar{\phi}}^s}{\partial t_M}=0\Rightarrow\dot{\alpha}_\theta=\dot{\bar{\bar{\gamma}}}^s sign(t_M)\\
&\frac{\partial\bar{\bar{L}}^s}{\partial\bar{\bar{q}}^s}=-\dot{\bar{\bar{\xi}}}^s+\dot{\bar{\bar{\gamma}}}^s\frac{\partial\bar{\bar{\phi}}^s}{\partial\bar{\bar{q}}^s}=0\Rightarrow\dot{\bar{\bar{\xi}}}^s=\dot{\bar{\bar{\gamma}}}^s\\
&\dot{\bar{\bar{\gamma}}}^s\ge 0,\ \ \bar{\bar{\phi}}^s\le 0,\ \ \dot{\bar{\bar{\gamma}}}^s\bar{\bar{\phi}}^s=0,\ \ \dot{\bar{\bar{\gamma}}}^s\dot{\bar{\bar{\phi}}}^s=0
\end{aligned} \tag{23}$$

For softening process at the discontinuity and elasticity process in the regular part of beam, we can write expression for final stress resultant value

$$t_{M,n+1}=E\left(\kappa_{n+1}^{(i)}-\kappa_n^p-\kappa_n^d-\tilde{G}^e\alpha_{n+1}\right)=\underbrace{E\left(\kappa_{n+1}^{(i)}-\kappa_n^p-\kappa_n^d-\frac{1}{l^e}\alpha_n\right)}_{t_{M,n+1}^{trial}}-\frac{E}{l^e}\underbrace{\left(\alpha_{n+1}-\alpha_n\right)}_{\dot{\bar{\gamma}}sign(t_{n+1}^{trial})} \tag{24}$$

2.1.4 Constitutive equations for shearing

Constitutive law for shearing of connection is defined as plasticity with linear hardening and nonlinear softening. Main ingredients for such a plasticity model are:

- additive decomposition of shear strain into elastic and plastic

$$\bar{\gamma}_s = \bar{\gamma}_s^e + \bar{\gamma}_s^p \tag{25}$$

- Helmholtz free energy

$$\begin{aligned} &\bar{\Psi}_s\left(\bar{\gamma}_s^e, \bar{\xi}_s^p\right) = \underbrace{\frac{1}{2}\bar{\gamma}_s^e G \bar{\gamma}_s^e}_{\bar{\Psi}^e} + \underbrace{\frac{1}{2}\bar{\xi}_s^p \bar{K}_{s,p} \bar{\xi}_s^p}_{\bar{\Xi}^p}; \bar{\bar{\Psi}}_s\left(\bar{\bar{\xi}}_s^s\right) = \frac{1}{2}\bar{\bar{\xi}}_s^s \bar{\bar{K}}_{s,s} \bar{\bar{\xi}}_s^s \\ &\Psi\left(\bar{\gamma}_s^e, \bar{\xi}_s^p, \bar{\bar{\xi}}_s^s\right) = \bar{\Psi}_s\left(\bar{\gamma}_s^e, \bar{\xi}_s^p\right) + \bar{\bar{\Psi}}_s\left(\bar{\bar{\xi}}_s^s\right)\delta_{\bar{x}}; \end{aligned} \tag{26}$$

where G is shear modulus, $\bar{\xi}^p, \bar{\xi}^s$ are internal hardening and softening variables, $\bar{K}_{s,p}$ is hardening modulus and $\bar{\bar{K}}_{s,s}$ is softening modulus.

- the plastic dissipation produced by this model, must be remain non-negative. That can be written as

$$0 \le \bar{\mathcal{D}}_s^p = \underbrace{V\left(\frac{\partial \bar{\psi}^e}{\partial V} - \bar{\gamma}_s^e\right)}_{\bar{\mathcal{D}}_s^e = 0} + V\dot{\bar{\gamma}}_s^p - \frac{\partial \bar{\bar{\Xi}}^p}{\partial \bar{\xi}^p}\dot{\bar{\xi}}^p \tag{27}$$

- yield functions for shearing

$$\bar{\phi}^p\left(V, \bar{q}_s^p\right) = |V| - \left(V_y - \bar{q}_s^p\right) \le 0 \tag{28}$$

where $V_y > 0$ denotes the yield shear force.

- The principle of maximum plastic dissipation which states that among all the variables $(V, \bar{q}_s^p)$ that satisfy the yield criteria $\bar{\phi}^p\left(V, \bar{q}_s^p\right)$ we ought to choose those that maximize plastic dissipation. This can be written as a constrained minimization problem

$$\min_{\sigma, \bar{q}^p} \max_{\dot{\bar{\gamma}}^p} \left[\bar{L}^p(V, \bar{q}_s^p, \dot{\bar{\gamma}}^p) = -\bar{\mathcal{D}}^p(V, \bar{q}_s^p) + \dot{\bar{\gamma}}^p \cdot \bar{\phi}^p(V, \bar{q}_s^p)\right] \tag{29}$$

where $\dot{\bar{\gamma}}^p \ge 0$ plays the role of Lagrange multiplier. By using the Kuhn-Tucker optimality conditions, the last result can provide the evolution equations for internal variables along with the loading/unloading conditions

$$\begin{aligned} &\frac{\partial \bar{L}^p}{\partial V} = -\dot{\bar{\gamma}}_s^p + \dot{\bar{\gamma}}^p \frac{\partial \bar{\phi}}{\partial V} = 0 \Rightarrow \dot{\bar{\gamma}}_s^p = \dot{\bar{\gamma}}^p sign(V) \\ &\frac{\partial \bar{L}^p}{\partial \bar{q}_s^p} = -\dot{\bar{\xi}}_s^p + \dot{\bar{\gamma}}^p \frac{\partial \bar{\phi}}{\partial \bar{q}_s^p} = 0 \Rightarrow \dot{\bar{\xi}}_s^p = \dot{\bar{\gamma}}^p \\ &\dot{\bar{\gamma}}^p \ge 0, \ \bar{\phi}^p \le 0, \ \dot{\bar{\gamma}}^p \bar{\phi}^p = 0 \end{aligned} \tag{30}$$

- The correct value of plastic multiplier can be computed from the consistency condition:

$$0<\dot{\bar{\gamma}}^{p};\ \ \bar{\phi}^{p}=0;\ \ \dot{\bar{\phi}}^{p}=0\ \Rightarrow\ \dot{\bar{\gamma}}^{p}=\frac{\frac{\partial\bar{\phi}^{p}}{\partial V}G\dot{\bar{\gamma}}_{s}}{\frac{\partial\bar{\phi}^{p}}{\partial V}G\frac{\partial\bar{\phi}^{p}}{\partial V}-\frac{\partial\bar{\phi}^{p}}{\partial\bar{q}^{p}}\frac{\partial\bar{q}^{p}}{\partial\bar{\xi}^{p}}\frac{\partial\bar{\phi}^{p}}{\partial\bar{q}^{p}}} \tag{31}$$

The remaining model ingredients define the softening response:

- The yield criteria for plasticity at the discontinuity can then be written

$$\bar{\bar{\phi}}(t_V,\bar{\bar{q}}_s^{\,p})=\left|t_V\right|-\left(t_{V_y}-\bar{\bar{q}}_s^{\,p}\right)\le 0 \tag{32}$$

where t_V is shearing traction, t_{V_y} is yield shearing traction and $\bar{\bar{q}}_s^{\,p}(\bar{\bar{\xi}}^{p})$ is softening shear stress variable at the discontinuity x_d.

- The principle of maximum plastic dissipation at discontinuity states that among all the variables $(t_V,\bar{\bar{q}}_s^{\,s})$ that satisfy the yield criteria $\bar{\bar{\phi}}_s^{s}\left(t_V,\bar{\bar{q}}_s^{\,s}\right)$ we choose those that maximize plastic dissipation. This can be written as a constrained minimization problem

$$\min_{t_V,\bar{\bar{q}}_s^{\,s}}\max_{\dot{\bar{\bar{\gamma}}}^{p}}\left[\bar{\bar{L}}^{s}(t_V,\bar{\bar{q}}_s^{\,s},\dot{\bar{\bar{\gamma}}}^{s})=-\bar{\bar{\mathcal{D}}}^{s}(t_V,\bar{\bar{q}}_s^{\,s})+\dot{\bar{\bar{\gamma}}}^{s}\cdot\bar{\bar{\phi}}_s^{s}(t_V,\bar{\bar{q}}_s^{\,s})\right] \tag{33}$$

where $\dot{\bar{\bar{\gamma}}}^{s}$ plays the role of Lagrange multiplier, $\bar{\bar{\mathcal{D}}}^{s}=\bar{\bar{q}}_s^{\,s}\dot{\bar{\bar{\xi}}}^{s}$ is dissipation of the energy in the softening process. By using the Kuhn-Tucker optimality conditions, the last result can provide the evolution equations for internal variables along with loading/unloading conditions

$$\begin{aligned}
&\frac{\partial\bar{\bar{L}}^{s}}{\partial t_V}=-\dot{\alpha}_{\gamma}+\dot{\bar{\bar{\gamma}}}^{s}\frac{\partial\bar{\bar{\phi}}}{\partial t_V}=0\Rightarrow\dot{\alpha}_{\gamma}=\dot{\bar{\bar{\gamma}}}^{s}sign(t_V)\\
&\frac{\partial\bar{\bar{L}}^{s}}{\partial\bar{\bar{q}}_s^{\,s}}=-\dot{\bar{\bar{\xi}}}^{s}+\dot{\bar{\bar{\gamma}}}^{s}\frac{\partial\bar{\bar{\phi}}}{\partial\bar{\bar{q}}_s^{\,s}}=0\Rightarrow\dot{\bar{\bar{\xi}}}^{s}=\dot{\bar{\bar{\gamma}}}^{s}\\
&\dot{\bar{\bar{\gamma}}}^{s}\ge 0,\ \ \bar{\bar{\phi}}^{s}\le 0,\ \ \dot{\bar{\bar{\gamma}}}^{s}\bar{\bar{\phi}}^{s}=0
\end{aligned} \tag{34}$$

2.1.5 Finite element implementation

The finite element formulation is practically same as formulation for the Timoshenko beam (e.g., Bui *et al*. 2014). In this section we present only the difference between these two elements.

The finite element implementation of the model is based upon the incompatible mode method (e.g., Ibrahimbegovic and Wilson 1991). The use of such a technique ensures that the enrichment with a generalized displacement jump remains local, with no additional degrees of freedom required at the global level. We consider the standard two-node Timoshenko beam and modified beam finite element interpolations, with linear polynomials as shape functions

$$N_1(x)=1-\left(x/L^{e}\right);N_2(x)=x/L^{e} \tag{35}$$

Standard interpolation of displacements at the continuous part can be written

$$\begin{aligned} u^h(x) &= N_1(x)u_1 + N_2(x)u_2 \\ v^h(x) &= N_1(x)v_1 + N_2(x)v_2 \\ \theta^h(x) &= N_1(x)\theta_1 + N_2(x)\theta_2 \end{aligned} \tag{36}$$

where u_a , v_a , θ_a are nodal values of generalized displacements and $N_a(x)$ is the interpolation function for node "a".

Thus, the corresponding interpolation of strain regular field for the modified Timoshenko beam can be written

$$\left.\begin{aligned} \varepsilon_N^h &= \frac{du^h}{dx} = B_1(x)u_1 + B_2(x)u_2 \\ \gamma^h &= \frac{dv^h}{dx} = B_1(x)v_1 + B_2(x)v_2 \\ \kappa^h &= \frac{d\theta^h}{dx} = B_1(x)\theta_1 + B_2(x)\theta_2 \end{aligned}\right\} \rightarrow \boldsymbol{\varepsilon}^h = \mathbf{Bd} \tag{37}$$

where

$$\begin{aligned} \mathbf{B} &= \begin{bmatrix} B_1 & 0 & 0 & B_2 & 0 & 0 \\ 0 & B_1 & 0 & 0 & B_2 & 0 \\ 0 & 0 & B_1 & 0 & 0 & B_2 \end{bmatrix};\ B_a = \frac{dN_a(x)}{dx} \\ \mathbf{d}^T &= \begin{bmatrix} u_1 & v_1 & \theta_1 & u_2 & v_2 & \theta_2 \end{bmatrix} \end{aligned} \tag{38}$$

We note that the choice we made herein is different from the standard interpolation of strain Timoshenko beam, recall that the latter can be written

$$\left.\begin{aligned} \varepsilon_N^h &= \frac{du^h}{dx} = B_1(x)u_1 + B_2(x)u_2 \\ \gamma^h = \frac{dv^h}{dx} &= B_1(x)v_1 + B_2(x)v_2 - N_1(x)\theta_1 - N_2(x)\theta_2 \\ \kappa^h &= \frac{d\theta^h}{dx} = B_1(x)\theta_1 + B_2(x)\theta_2 \end{aligned}\right\} \rightarrow \boldsymbol{\varepsilon}^h = \mathbf{Bd} \tag{39}$$

where

$$\begin{aligned} \mathbf{B} &= \begin{bmatrix} B_1 & 0 & 0 & B_2 & 0 & 0 \\ 0 & B_1 & -N_1 & 0 & B_2 & -N_2 \\ 0 & 0 & B_1 & 0 & 0 & B_2 \end{bmatrix} \\ \mathbf{d}^T &= \begin{bmatrix} u_1 & v_1 & \theta_1 & u_2 & v_2 & \theta_2 \end{bmatrix} \end{aligned} \tag{40}$$

This different interpolation of the strains we choose herein produces uncoupling between transverse displacement and bending moment. Details of the finite element formulation and computational procedure were presented in (Bui *et al*. 2014).

3. Identification procedure for model parameters

In the case of connection testing, the global response of a specimen can be represented in terms of load-displacement *F-u* diagram. Any such curve can be related to three-phases of the connection response: elastic, hardening and softening part (Fig. 3). Model for hardening behavior of the connection is defined as coupled plasticity-damage while the softening response is governed by nonlinear law. For the most general case, in the elastic phase, we need to identify four parameters, whereas in the hardening phase eight and in the softening phase another six parameters.

The identification in general case is performed in two steps: i) definition of an objective function based on some experimental measurements; ii) minimization of this objective function in order to find values of constitutive parameters used in the model.

The choice of objective function is very important step, to ensure the success of the minimization. In general case, objective function can be defined as gap between measured and computed response values (displacement, stress, deformation, reaction force and etc.)

$$J(\mathbf{d}_{\mathrm{p}}) = \sum_{j \in J} n\left(\mathbf{u}_j^{com}(\mathbf{d}_{\mathrm{p}}) - \mathbf{u}_j^{\exp}\right)^2 \tag{41}$$

where $\mathbf{d}_{\mathrm{p}}$ are the model parameters that we seek to identify or similar, $\mathbf{u}_j^{com}(\mathbf{d}_{\mathrm{p}})$ and $\mathbf{u}_j^{\exp}$ are, respectively, computed and experimentally measured values of displacements/stresses/strains and n is weighting factor for different terms of objective function. Coupled plasticity – damage model is complex for identification because both plasticity and damage can represent same behavior during the loading process. However, we can find difference in the unloading process. For that reason, the objective function in the hardening phase needs to contain information from unloading process.

Minimization of the objective function can formally be written as minimization under constraint

$$\min_{G(\sigma;\delta w)=0} J(\mathbf{d}_{\mathrm{p}}) = \sum_{j \in J} n\left(\mathbf{u}_j^{com}(\mathbf{d}_{\mathrm{p}}) - \mathbf{u}_j^{\exp}\right)^2 \tag{42}$$

where the weak form of equilibrium equations $G(\varepsilon, \zeta^p, \zeta^d; \delta w) = 0$ is the corresponding constraint. Namely, the weak form of equilibrium equations has to be satisfied at every moment. The constrained minimization of objective function can be transferred into unconstrained minimization by using Lagrange multiplier method (e.g., Ibrahimbegovic *et al*. 2004)

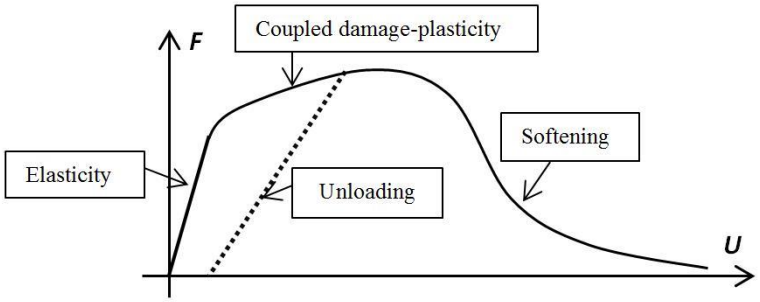

Fig. 3 Curve force *F* – displacement *U*

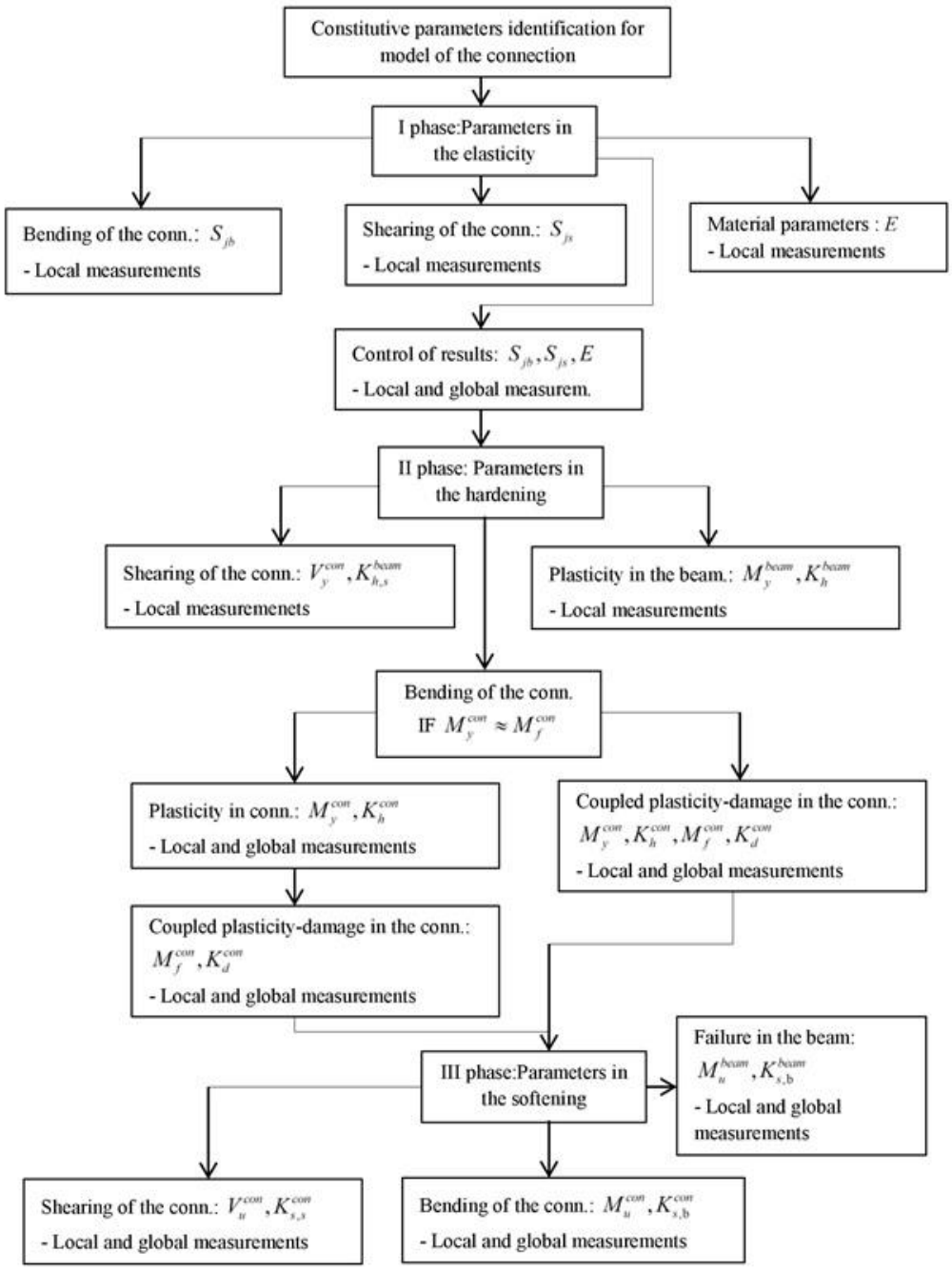

Fig. 4 Flow chart of parameters identification

$$\max_{\forall\lambda}\min_{G(\sigma;\mathbf{d}_p)=0} L(\sigma,\mathbf{d}_{\mathrm{p}},\lambda)=J(\mathbf{d}_p)+\mathrm{G}(\sigma,\mathbf{d}_{\mathrm{p}},\lambda) \tag{43}$$

where λ are Lagrange multipliers inserted into the weak form of equilibrium equations instead of virtual displacement. This type of minimization of the objective function is very complex for eighteen unknowns.

Such an unconstrained minimization of the objective function is split in several phases, in every phases number of unknowns decreases to maximal of four parameters.

The general identification procedure of the connection model parameters is presented in the flowchart in Fig. 4. The process is split in three phases, with every phase further split to few cases. For every case, local and global measurements are required.

Local measurements depend only on one constitutive model, while the global ones depend on all models. This objective function is defined in detail for different cases of identification, in the first example, where experimental results are replaced by those obtained from FEM model.

Unconstrained minimization methods included in Matlab are used to solve the identification problem. In particular, we use four methods: BFGS (Broyden–Fletcher–Goldfarb–Shanno method), DFP (Davidon–Fletcher–Powell method), Trust Region and Steepest Descent. The comparisons between these methods are presented in the examples that follow.

Objective function for parameters identification of the connection for the general case can be written as

$$\begin{aligned} J\left(\mathbf{d}_p\right)=&\sum_1^3 a\left(F_{Pi}^{com}-F_{Pi}^{\exp}\right)^2+\sum_1^3 b\left(U_{Pi}^{com}-U_{Pi}^{\exp}\right)^2+\sum_1^3 b\left(U_{S,Pi}^{com}-U_{S,Pi}^{\exp}\right)^2+\sum_1^3 c\left(\theta_{Pi}^{com}-\theta_{Pi}^{\exp}\right)^2+\\ &+\sum_1^3 c\left(\theta_{Pi'}^{com}-\theta_{Pi'}^{\exp}\right)^2+\sum_1^2 d\left(\Delta\theta_{Pi}^{com}-\Delta\theta_{Pi}^{\exp}\right)^2+\sum_1^3 e\left(\kappa_{Pi}^{com}-\kappa_{Pi}^{\exp}\right)^2+\sum_1^3 e\left(\kappa_{Pi'}^{com}-\kappa_{Pi'}^{\exp}\right)^2+\\ &+\sum_1^3 g\left(\Delta\kappa_{Pi}^{com}-\Delta\kappa_{Pi}^{\exp}\right)^2 \end{aligned} \tag{44}$$

where are: $F_{Pi}^{com},F_{Pi}^{\exp}$ - forces for different load level ($\mathrm{P_i}$); $U_{Pi}^{com},U_{Pi}^{\exp}$ - displacements ($\mathrm{P_i}$); $U_{S,Pi}^{com},U_{S,Pi}^{\exp}$ - shear displacements ($\mathrm{P_i}$); $U_{Pi'}^{com},U_{Pi'}^{\exp}$ - residual displacements (unloaded point $\mathrm{P_{i'}}$); $\theta_{Pi}^{com},\theta_{Pi}^{\exp}$ - rotations of the connection ($\mathrm{P_i}$); $\theta_{Pi'}^{com},\theta_{Pi'}^{\exp}$ - residual rotations (unloaded point $\mathrm{P_{i'}}$); $\Delta\theta_{Pi}^{com}=\theta_{Pi+1}^{com}-\theta_{Pi}^{com}$ and $\Delta\theta_{Pi}^{\exp}=\theta_{Pi+1}^{\exp}-\theta_{Pi}^{\exp}$ - gradients of rotation between two different load ($\mathrm{P_i}$); $\kappa_{Pi}^{com},\kappa_{Pi}^{\exp}$ - curvatures of the section ($\mathrm{P_i}$); $\kappa_{Pi'}^{com},\kappa_{Pi'}^{\exp}$ - residual curvatures of the section (unloaded point $\mathrm{P_{i'}}$); $\Delta\kappa_{Pi}^{com}=\kappa_{Pi+1}^{com}-\kappa_{Pi}^{com}$ and $\Delta\kappa_{Pi}^{\exp}=\kappa_{Pi+1}^{\exp}-\kappa_{Pi}^{\exp}$ - gradients of curvature between two different load ($\mathrm{P_i}$); a, b, c, d, e, g - constants

4. Numerical examples

In this work we present three numerical examples in order to illustrate the performance of proposed approach. First example serves to illustrate all cases of identification, where the corresponding experimental results are obtained from fine FEM model. The remaining two examples provide the illustration procedure for identification of model parameters for real experimental results of the steel connection and the timber connection. Moreover, the examples serve to illustrate that proposed identification procedure applies to parameters identifications in

steel and in timber structures, the cases of large practical interest.

4.1 Steel structure connection with complete set of failure modes

In this example we present methodology for identification parameters which describes nonlinear behavior of both connection and structural members. We need to obtain eighteen unknowns in total. Measurement values in this example were computed by a more refined mesh of beam elements. We practically can test all phases for proposed identification procedure.

4.1.1 Experimental setup and FEM model

In Fig. 5 are shown experimental setup for testing connection between two orthogonal steel beams and corresponding FEM model. The horizontal beam is chosen much stronger then the vertical beam, which should ensure the linear elastic behavior of horizontal beam during the test. The equipment for displacements and deformations measurements is arranged so that gives us sufficient information for identification of mechanical properties. The results can be classified as local and global measurements. The global measurements depend on all model parameters, while the local measurements depend on only one model parameter.

In particular, the measuring equipment illustrated in Fig. 5 consists of: LVDT (*Linear variable displacement transducer*) 1 and 2, which measure global displacements of the vertical beam in node 3 ($U_{3,Pi}^{\exp}$) and node 5 ($U_{5,Pi}^{\exp}$); LVDT 3 and 4, which measure relative vertical displacement between horizontal and vertical beams, which the latter used for calculating rotation of the connection

$$\theta^{\exp} = \frac{\Delta v_3^{\exp} - \Delta v_4^{\exp}}{h_{vert.beam}} \tag{45}$$

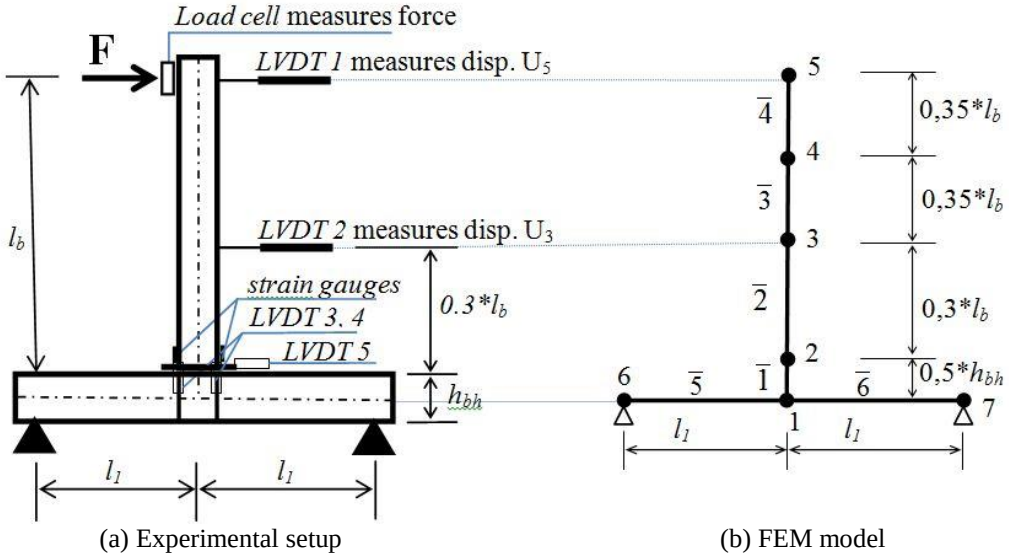

(a) Experimental setup (b) FEM model

Fig. 5 Experimental setup and FEM model

LVDT 5, which measurs relative horizontal displacement ($U^{\exp}_{2,Pi} = U^{\exp}_{S,Pi}$) between horizontal and vertical beams, which measures transverse(shearing) displacement of connection; Strain guges measure deformation at the vertical beam. The latter is used for calculating the curvature of the section near to connection, assuming the vertical beam is not loaded with axial force

$$\varepsilon_i^{\exp} = -y \cdot \kappa_i \Rightarrow \kappa_i = -\frac{\varepsilon_i^{\exp}}{y};\ y = \left[-\frac{h}{2}, \frac{h}{2}\right] \Rightarrow \kappa^{\exp} = \frac{\kappa_1 + \kappa_2}{2} \tag{46}$$

All the measurments can be taken continuously during the test.

The FEM model is composed of six frame elements. Element number 1 was used for modeling connection as described in Section 2.1., while all other elements (2,3,4,5,6) are chosen as the Euler-Bernoulli beams.

4.1.2 Phase I of elastic parameters identification (S_{jb},S_{js}, E)

In this phase we need to identify three parameters governing elastic response: S_{jb} is stiffness of connection for bending, S_{js} is stiffness of connection for shearing and E is modulus of elasticity for steel beams.

Modulus of elasticity E for steel beam can be obtained using the standard material tests. Alternatively, the modulus E can be identified from local measurement of strain gauges, separately of the other measurements. The shearing stiffness of connection (S_{js}) can be obtained from local measurement of LVDT 5. The bending stiffness of connection (S_{ib}) can be identified from local measurement rotations of connection.

Loading program for this phase is presented at the Fig, 6. In the time (points: a',b',c') we measure residual (plastic) displacement, if these measurements are equal to zero then plasticity is not activated yet.

By using only measurements of rotation, we can identify stiffness of connection in elasticity (for virgin material). In this identification, we use relation between elasticity and damage stiffness of connection

$$S^e_{jb} = \frac{1}{S^d_{jb}} \tag{47}$$

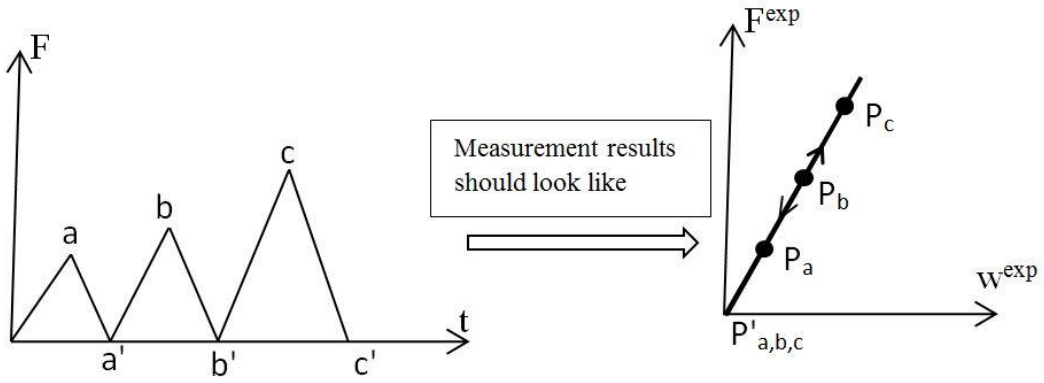

Fig. 6 Loading program and measurements in the elasticity

where S_{jb}^{e}, S_{jb}^{d} are stiffness coefficients of linear-elastic and of damage model. This relation allows us to reduce identification procedure to one parameter.

The objective function for the identification properties for elastic bending of the connection can be written as

$$J\left(S_{jb}^{e}, S_{jb}^{d}\right) = \sum_{1}^{3}\left(\theta_{Pi}^{com} - \theta_{Pi}^{\exp}\right)^{2} \tag{48}$$

The shearing stiffness of the connection can be obtained from local measurements of LDVT5, where we measure relative displacement between horizontal and vertical beam, which is triggered by sliding of connection. The objective function for this identification can be written as

$$J\left(S_{js}^{e}\right) = \sum_{1}^{3}\left(U_{2,Pi}^{com} - U_{2,Pi}^{\exp}\right)^{2} \tag{49}$$

Modulus of elasticity of steel beam can be obtained from local measurements of strain gauges. The objective function is now defined as

$$J\left(E^{beam}\right) = \sum_{1}^{3}\left(\kappa_{Pi}^{com} - \kappa_{Pi}^{\exp}\right)^{2} \tag{50}$$

At the end of this phase we can control results of identification using combination of local and global measurements and identify all parameters simultaneously. A universal objective function can be written

$$\begin{aligned} J\left(S_{jb}^{e}, S_{jb}^{d}, S_{js}^{e}, E^{beam}\right) = & \sum_{1}^{3}\left(U_{5,Pi}^{com} - U_{5,Pi}^{\exp}\right)^{2} + \sum_{1}^{3}\left(U_{3,Pi}^{com} - U_{3,Pi}^{\exp}\right)^{2} \\ & + \sum_{1}^{3} c\left(\theta_{Pi}^{com} - \theta_{Pi}^{\exp}\right)^{2} + \sum_{1}^{3} d\left(k_{Pi}^{com} - k_{Pi}^{\exp}\right)^{2} \end{aligned} \tag{51}$$

where *c* and *d* are constants defining the weights of global and local displacement measurements. Global measurements typically have significantly bigger weights than local.

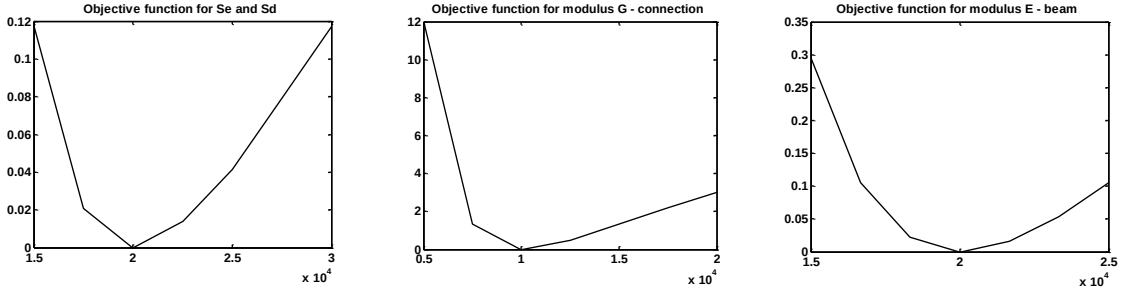

(a) OF: $J\left(S_{jb}^{e}, S_{jb}^{d}\right)$ (b) OF: $J\left(S_{js}^{e}\right)$ (c) OF: $J\left(E^{beam}\right)$

Fig. 7 Objective functions

4.1.3 Phase II of identification procedure for coupled plasticity-damage model constitutive parameters

In this phase we need to identify eight parameters: M_y^{con} - bending moment of plastic yielding of the connection; $K_{b,h}^{con}$ - plastic hardening modulus for bending of the connection; M_f^{con} - bending moment of damage yielding of the connection; K_d^{con} - damage hardening modulus for bending of the connection; V_y^{con} - shearing force of plastic yielding of the connection; $K_{s,h}^{con}$ - plastic hardening modulus for shearing of the connection; M_y^{beam} - bending moment of plastic yielding of the beam; K_h^{beam} - plastic hardening modulus for bending of the beam. For identification procedure these parameters can be divided in three groups: beam parameters (M_y^{beam}, K_h^{beam}), shearing in connection ($V_y^{con}, K_{s,h}^{con}$) and bending in connection ($M_y^{con}, K_{b,h}^{con}, M_f^{con}, K_d^{con}$).

Plasticity model for beam failure

The parameters for plasticity model for beam failure can be obtained from local measurements by strain gauges. The strain gauges are providing the measurements all along the loading program. When the plasticity is activated, we need to have values of deformation for three loading-unloading cycles.

The identification can be completed successfully with this kind of measurements. Objective function for this identification can be written

$$J\left(K_h^{beam}, M_y^{beam}\right) = \sum_1^3 \left(k_{Pi}^{com} - k_{Pi}^{\exp}\right)^2 + \sum_1^3 \left(k_{Pi}^{com} - k_{Pi}^{\exp}\right)^2 + \sum_1^2 \left(\Delta k_{Pi}^{com} - \Delta k_{Pi}^{\exp}\right)^2 \tag{52}$$

The objective function is shown in Fig. 9(a), we can see that function is convex, which allows to easily obtain its minimum. The minimization of the objective function was done using different methods: BFGS, DFP, Trust Region and Steepest Descent. Comparison of efficiency of these methods is presented in Table 1

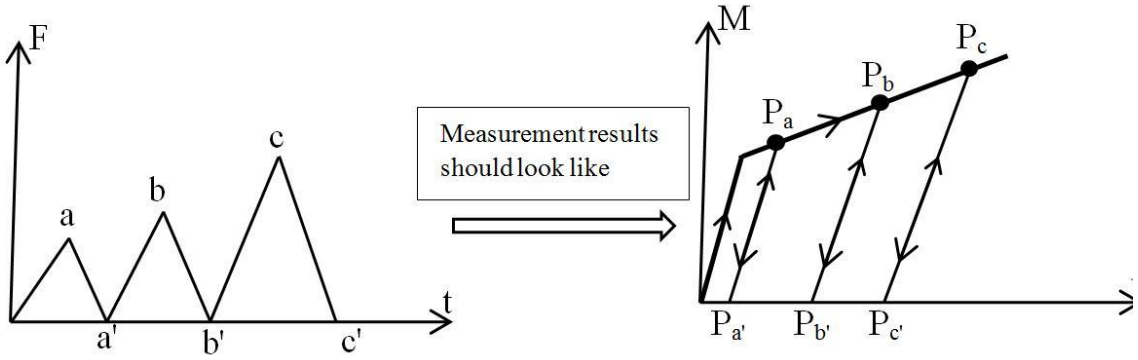

Fig. 8 Loading program and results of measurings in the plasticity

Table 1 Efficiency of different methods for minimization of $J\left(K_h^{beam}, M_y^{beam}\right)$

Applied method for minimization	Number of		Time of computation	Max. error of the Identification [%]
	Iterations	Evolutions		
BFGS	11	21	50 s	0,00
DFP	45	57	95 s	0,00
Trust Region	22	23	125 s	0,00
Steepest Descent	5	48	108 s	12,55

Table 2 The efficiency of different methods for minimization of $J\left(F_y, K_{hs}^{con}\right)$

Applied Method for minimization	Number of		Time of computation	Max. error of the Identification [%]
	Iterations	Evolutions		
BFGS	13	19	34 s	0,10
DFP	16	45	75 s	3,35
Trust Region	171	171	780 s	0,59
Steepest Descent	37	150	380 s	0,04

Plasticity model for shearing of the connection

Parameters of the plasticity model for shearing of the connection can be identified from local measurement LVDT 5. In this part we use analogy in the loading program which has presented in this paper. More precisely, the loading program and expected results of measuring look same as presented. The chosen objective function can be written

$$J\left(F_y, K_{hs}^{con}\right) = \sum_{1}^{3}\left(U_{2,Pi}^{com} - U_{2,Pi}^{\exp}\right)^2 + \sum_{1}^{3}\left(U_{2,Pi}^{com} - U_{2,Pi}^{\exp}\right)^2 + \sum_{1}^{2}\left(\Delta U_{2,Pi}^{com} - \Delta U_{2,Pi}^{\exp}\right)^2 \tag{53}$$

The shape of this objective function we can see in Fig. 9(b). This function is convex and has a minimum. Results of comparison among different methods for minimization of this function are presented in Table 2.

Coupled-plasticity model for bending deformation of the connection

Parameters of the coupled-plasticity model for bending of the connection can be obtained from all measurements. This task is the most complex, where we need to have measurements at both global and local levels, as well as previously identified values ($V_y^{con}, K_{s,h}^{con}, M_y^{beam}, K_h^{beam}$). Here we can have two different cases. In the first case, the value of damage moment is significantly larger than yielding moment. The second case, both bending moments have close values.

The first case is simpler for identification, because we can identify parameters for plasticity first and then for damage model. We consider having this case when minimum three cycles occur with typical plasticity type response (unloading lines parallel with first loading line). The measured values should look like those in diagram in Fig. 10.

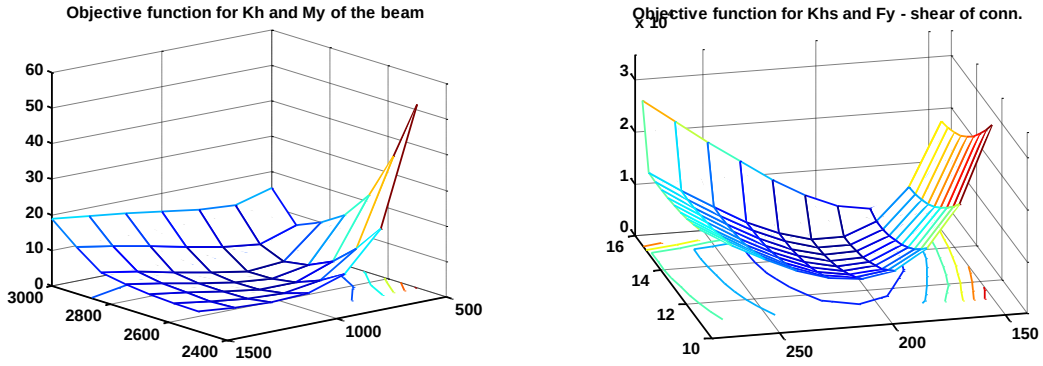

(a) OF: $J\left(K_h^{beam}, M_y^{beam}\right)$ (b) OF: $J\left(F_y, K_{hs}^{con}\right)$

Fig. 9 Shapes of Objective functions

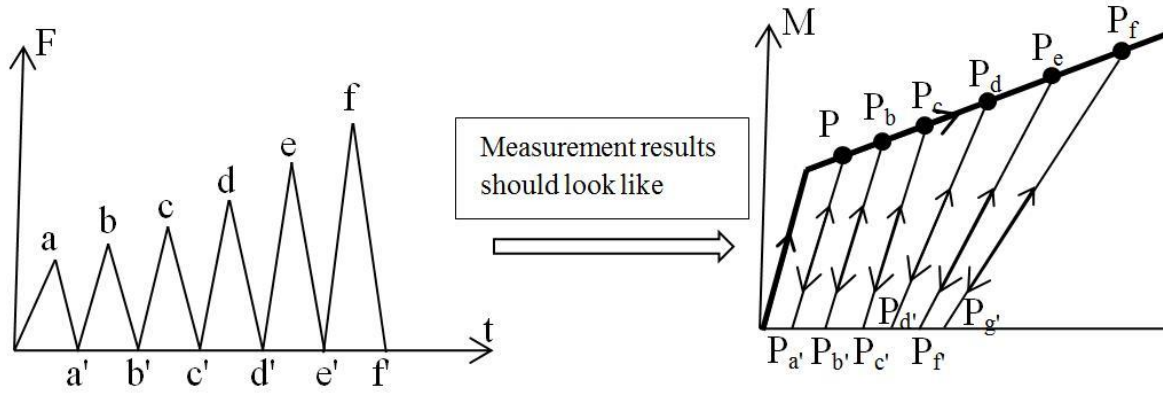

Fig. 10 Loading program and results of measurements in the coupled plasticity-damage

Objective function for identification of parameters of plasticity models for connection can be written as

$$J\left(K_{h,b}^{con}, M_y^{con}\right) = \sum_1^3 \left(U_{5,Pi}^{com} - U_{5,Pi}^{\exp}\right)^2 + \sum_1^3 \left(U_{3,Pi}^{com} - U_{3,Pi}^{\exp}\right)^2 + \sum_1^3 m\left(\theta_{Pi}^{com} - \theta_{Pi}^{\exp}\right)^2 + \sum_1^3 m\left(\theta_{Pi'}^{com} - \theta_{Pi'}^{\exp}\right)^2 + \sum_1^2 n\left(\Delta\theta_{Pi}^{com} - \Delta\theta_{Pi}^{\exp}\right)^2 \tag{54}$$

The shape of objective function is shown in Fig. 12(a). This surface is convex and it can easily be minimized. The minimization is done by using four different methods. The comparison of the results is shown in Table 3.

Table 3 Efficiency of different methods for minimization of $J\left(M_y^{con}, K_{h,b}^{con}\right)$

Applied Method for minimization	Number of		Time of computation	Max. error of the Identification [%]
	Iterations	Evolutions		
BFGS	12	27	53 s	0,00
DFP	39	51	91 s	0,00
Trust Region	71	72	402 s	1,33
Steepest Descent	13	69	120 s	14,80

Table 4 Efficiency of different methods for minimization of $J\left(M_f^{con}, K_d^{con}\right)$

Applied Method for minimization	Number of		Time of computation	Max. error of the Identification [%]
	Iterations	Evolutions		
BFGS	14	29	64 s	0,00
DFP	50	66	137 s	0,00
Trust Region	34	35	231 s	10,14
Steepest Descent	9	48	87 s	20,75

Afterward, we start identification of parameters for damage model (M_f^{con}, K_d^{con}), where the previously identified parameters for plasticity are kept. The identification problem is reduced to two parameters. The objective function is same, while only load level is different therefore we use measured values from last three cycles (Fig. 10).

This objective function is convex and we can see shape in Fig. 12(b). The minimization is done using four different methods. The efficiency of these methods is presented in Table 4.

The second case is the most complex, the identification can't be split in two parts. The damage moment and the yielding moment have close values (Fig. 11) and we need to identify four parameters simultaneously. The identification of four parameters is possible with the same objective function, where we use results of local and global measurements. The efficiency and the accuracy in minimization process depend on first guest values, if we have good start values we can obtain parameters with acceptable errors. Results of the minimization objective function for four unknowns with four different methods are presented in the Table 5. In this minimization we used start values, which are not close to correct values. From these results we can conclude that only BFGS method gives results with acceptable errors (*2,79 < 3%*).

Table 5 Efficiency of different methods for minimization of $J\left(M_y^{con}, K_{h,b}^{con}, M_f^{con}, K_d^{con}\right)$

Applied Method for minimization	Number of		Time of computation	Max. error of the Identification [%]
	Iterations	Evolutions		
BFGS	25	54	161 s	2,79
DFP	58	97	289 s	13,62
Trust Region	81	82	1333 s	6,05
Steepest Descent	22	96	290 s	9,25

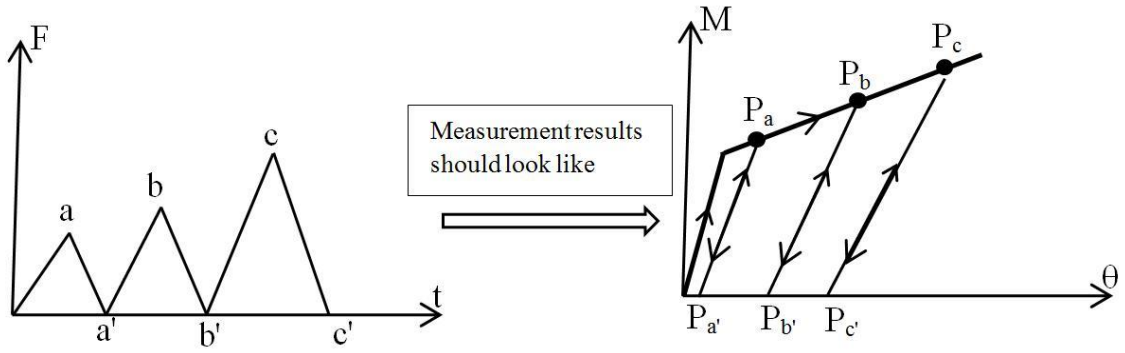

Fig. 11 Loading program and results of measurements in the coupled plasticity-damage

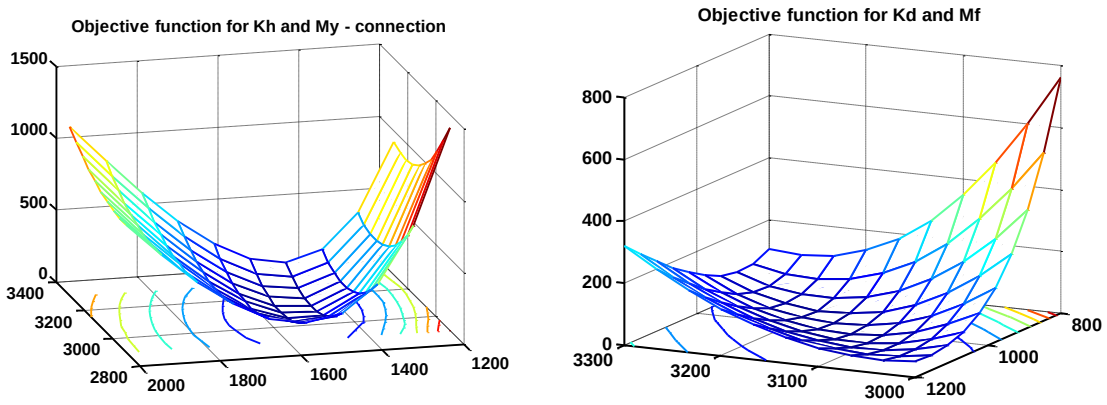

(a) OF: $J\left(M_y^{con}, K_{h,b}^{con}\right)$ (b) OF: $J\left(M_f^{con}, K_d^{con}\right)$

Fig. 12 Shapes of Objective functions

To reduce these errors we can make control identification two by two parameters. First, we can identify parameters for plasticity model ($M_y^{con}, K_{h,b}^{con}$), while damage parameters are taken as known. Afterword, parameters for the damage model ($M_f^{con}, K_{d,b}^{con}$) are unknown and for the plasticity known. In these two control identifications were determined practically same values of model parameters, but all methods for minimization gave us acceptable errors.

4.1.4 Phase III of identification procedure for softening model constitutive parameters

In this phase six parameters can be actived: M_u^{con} - ultimate bending moment of the connection; $G_{f,b}^{con}$ - fracture energy for bending of the connection; V_u^{con} - ultimate shearing force of the connection; $G_{f,s}^{con}$ - fracture energy for shearing of the connection; M_u^{beam} - ultimate bending moment of the beam; G_f^{beam} - fracture energy of the beam. These parameters can be

obtained in three different cases: failure for bending in the connection ($M_u^{con}, G_{f,b}^{con}$), failure for shearing in the connection ($V_u^{con}, G_{f,s}^{con}$) and failure in the steel beam ($M_u^{beam}, G_{f,b}^{beam}$).

Only one failure mechanism can happen. The local measurements are able to indicate which of the failure mechanism is activated. Failure for bending in connection can be noted from local measurements LVDT 3 and 4, while the failure for shearing in connection from LVDT5. The identification can be done for each of these cases.

First case – softening (failure) for bending in the connection

Objective function for this case is combination of local and global measurements. It can be written:

$$J\left(M_u^{con}, G_{f,b}^{con}\right) = \sum_1^4 \left(F_{5,Pi}^{com} - F_{5,Pi}^{\exp}\right)^2 + \sum_1^4 \left(U_{5,Pi}^{com} - U_{5,Pi}^{\exp}\right)^2 + \sum_1^4 m\left(\theta_{Pi}^{com} - \theta_{Pi}^{\exp}\right)^2 \tag{55}$$

The shape of this objective function is shown in Fig. 13(a). We can see, it is convex function and has minimum. The minimization was done with four methods. Results of the identification procedure are presented in Table 6.

Table 6 Efficiency of different methods for minimization of $J\left(M_u^{con}, G_{f,b}^{con}\right)$

Applied Method for minimization	Number of		Time of computation	Max. error of the Identification [%]
	Iterations	Evolutions		
BFGS	7	32	196 s	0,22
DFP	6	35	217 s	0,75
Trust Region	41	42	796 s	0,44
Steepest Descent	28	75	497 s	0,45

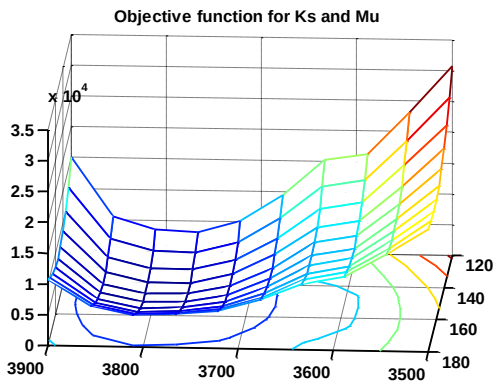

(a) Objective function $J\left(M_u^{con}, G_{f,b}^{con}\right)$

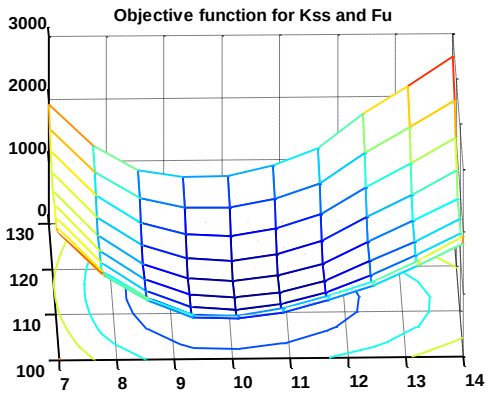

(b) Objective function $J\left(F_u^{con}, G_{f,s}^{con}\right)$

Fig. 13 Shapes of Objective functions

Table 7 The efficiency of different methods for minimization of $J\left(F_u^{con}, G_{f,\mathrm{s}}^{con}\right)$

Applied Method for minimization	Number of		Time of computation	Max. error of the Identification [%]
	Iterations	Evolutions		
BFGS	2	40	48 s	2,02
DFP	5	34	75 s	3,70
Trust Region	21	22	139 s	5,11
Steepest Descent	3	30	80 s	3,31

Second case – softening (failure) for shearing in the connection

Objective function for this case is combination of local and global measurements. It can be written

$$J\left(F_u^{con}, G_{f,\mathrm{s}}^{con}\right) = \sum_1^4 \left(F_{5,Pi}^{com} - F_{5,Pi}^{\exp}\right)^2 + \sum_1^4 \left(U_{5,Pi}^{com} - U_{5,Pi}^{\exp}\right)^2 + \sum_1^4 \left(U_{2,Pi}^{com} - U_{2,Pi}^{\exp}\right)^2 \tag{56}$$

The shape of this objective function is shown in Fig. 13(b). It is convex function and the minimization was done with four methods. In the Table 7, we can see that only BFGS method obtained results with acceptable errors.

Third case – softening (failure) in the steel beam

This failure mechanism is current if other have not activated. In this case, we can use only global measurements for identification softening parameters of steel beam. The local measurement of strain gauges isn't useful because we don't know where the hinge will be located.

$$J\left(F_u^{con}, G_{f,s}^{con}\right) = \sum_1^4 \left(F_{5,Pi}^{com} - F_{5,Pi}^{\exp}\right)^2 + \sum_1^4 \left(U_{5,Pi}^{com} - U_{5,Pi}^{\exp}\right)^2 \tag{57}$$

The shape of this objective function is shown in Fig. 14. This function is convex, but with small irregularities. These irregularities can be reduced, if we use more experimental results. In this work we used four time point (load level) and the identification procedure was successful.

Table 8 The efficiency of different methods for minimization of $J\left(M_u^{beam}, G_{f,\mathrm{b}}^{beam}\right)$

Applied Method for minimization	Number of		Time of computation	Max. error of the Identification [%]
	Iterations	Evolutions		
BFGS	5	27	47 s	0,75
DFP	7	35	68 s	0,70
Trust Region	20	21	146 s	0,88
Steepest Descent	5	31	61 s	0,95

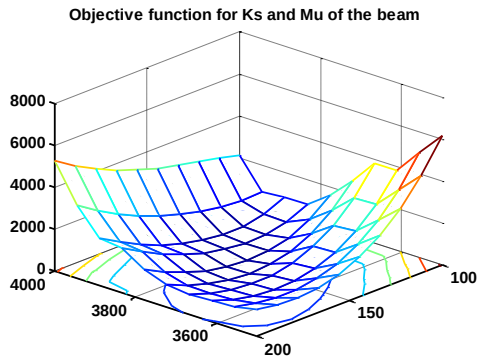

Fig. 14 The objective function $J\left(M_u^{beam}, G_{f,\mathrm{b}}^{beam}\right)$

4.2 Identification parameters of the steel connection in bending

The presented identification methodology was applied to the experimental results found in the literature. The corresponding hysteresis curve (e.g., Shi *et al*. 2005) was used for approximation of relation bending moment – rotation. For these experimental results we have tested presented methodology. The hysteresis curve of the end plate connection and approximation of test results are shown in Fig. 15.

The identification of model parameters starts with elastic phase, where we need to identify the bending stiffnesses of elasticity and damage model. Namely, coupled plasticity-damage model is composed of two serial connected models, so that the bending stiffness can be calculated as

$$\left.\begin{aligned} S_{j,b} &= \frac{S_{j,bp}S_{j,bd}^{-1}}{S_{j,bp}+S_{j,bd}^{-1}} \\ S_{j,bp} &= S_{j,bd}^{-1} \end{aligned}\right\} \rightarrow S_{j,b} = \frac{1}{2}S_{j,bp} \tag{58}$$

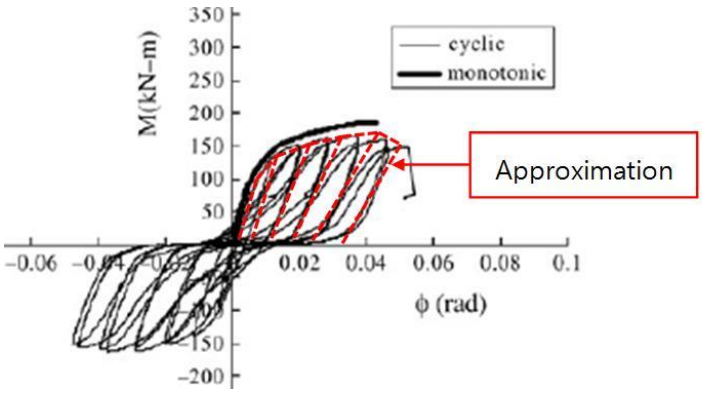

Fig. 15 Typical hysteresis curve and approximation of the test results

where S_{jb}^{e}, S_{jb}^{d} are stiffness of linear-elastic and damage model. This expression reduces identification to one parameter.

Objective function can be written

$$J\left(S_{jb}^{e}, S_{jb}^{d}\right) = \left(\theta_{P1}^{com} - \theta_{P1}^{\exp}\right)^2 \tag{59}$$

The objective function (Fig. 16(a)) is convex and parameters were identified successfully.

In the second phase of identification for coupled plasticity-damage model, we start with simultaneous identification of four parameters.

Objective function, which was used for the identification

$$J\left(K_{h,b}^{con}, M_{y}^{con}\ K_{d,b,}^{con}, M_{f}^{con}\right) = \sum_{1}^{3} m\left(\theta_{Pi}^{com} - \theta_{Pi}^{\exp}\right)^2 + \sum_{1}^{3} m\left(\theta_{Pi}^{com} - \theta_{Pi}^{\exp}\right)^2 + \sum_{1}^{2} n\left(\Delta\theta_{Pi}^{com} - \Delta\theta_{Pi}^{\exp}\right)^2 \tag{60}$$

The objective function is convex for all parameters and process was done successfully.

Control of these identified parameters was made in two split processes of the identification. First we identify two unknown for plasticity model while damage parameters are fixed and known. In the second cases we use analogy where two damage parameters are unknown and plasticity known. Shape of objective functions for both cases is presented in the Fig. 16.

Objective functions (Figs. 16(b) and 16(c)) are convex. These control results are matched with results of simultaneous identification for all parameters.

Results of identification are presented in Fig. 19(a) where we can see very good matching experimental and computed results. Computed results were obtained using FEM element model with identified constitutive parameters.

4.3 Identification parameters of the connection in Timber structure

In the second example, presented methodology was tested at the connection between two wood elements. Hysteresis curve (e.g., Mesic 2003) and approximation of experimental results are showed at the Fig. 17. This hysteresis curve was measured with big increment steps of displacement. In the middle of curve we can see gap without unloading measurings, but this enable to test quality of proposed methodology.

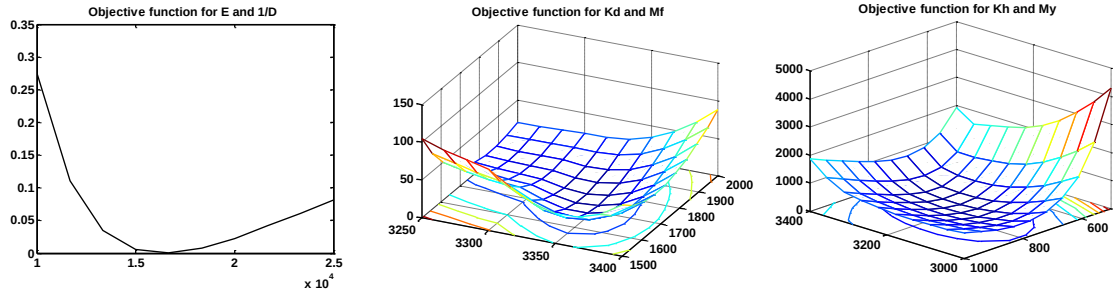

(a) OF: $J\left(S_{jb}^{e}, S_{jb}^{d}\right)$ (b) OF: $J\left(K_{d}^{con}, M_{f}^{con}\right)$ (c) OF: $J\left(K_{h}^{con}, M_{y}^{con}\right)$

Fig. 16 Shapes of Objective functions

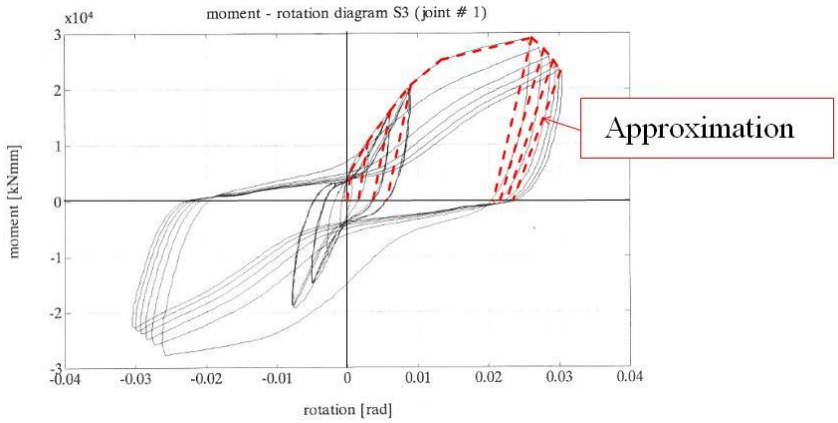

Fig. 17 Typical hysteresis curve and approximation of the test results

The identification of models parameters is started with elastic phase, same as last example. Objective function can be written (Fig. 18(a))

$$J\left(S_{jb}^{e}, S_{jb}^{d}\right) = \left(\theta_{P1}^{com} - \theta_{P1}^{\exp}\right)^2 \tag{61}$$

In second phase of identification for coupled plasticity-damage model, we start with simultaneous identification for four parameters.

The objective function can be written as

$$J\left(K_{h,b}^{con}, M_{y}^{con}\ K_{d,b,}^{con}, M_{f}^{con}\right) = \sum_{1}^{3} m\left(\theta_{Pi}^{com} - \theta_{Pi}^{\exp}\right)^2 + \sum_{1}^{3} m\left(\theta_{Pi}^{com} - \theta_{Pi}^{\exp}\right)^2 + \sum_{1}^{2} n\left(\Delta\theta_{Pi}^{com} - \Delta\theta_{Pi}^{\exp}\right)^2 \tag{62}$$

The objective function is convex for all parameters and process of identification is done successfully.

Same as in the last example, control of identified parameters was made in two split processes of the identification. First we have identified two unknowns for plasticity model while damage parameters were fixed and known. In this case objective function is good conditioned (Fig. 16(b)). In the second case objective function is convex but no so good conditioned, but with the good start values in the minimization we can obtain good results.

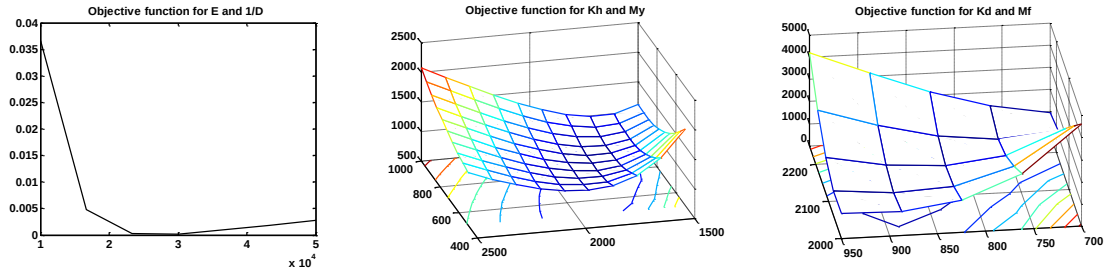

(a) OF: $J\left(S_{jb}^{e}, S_{jb}^{d}\right)$ (b) OF: $J\left(K_{h}^{con}, M_{y}^{con}\right)$ (c) OF: $J\left(K_{d}^{con}, M_{f}^{con}\right)$

Fig. 18 Shapes of Objective functions

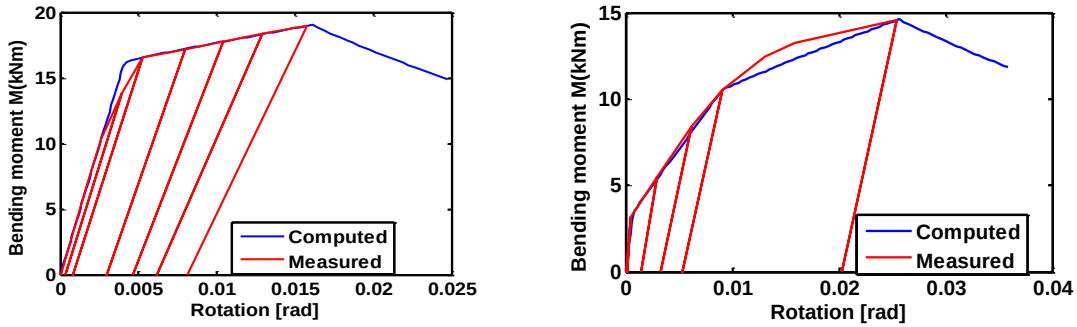

(a) Steel connection (b) Timber connection

Fig. 19 Matching results: experimental vs. computed

Results of identification are presented in the Fig. 19(b) where we can see good matching experimental and computed results. Computed results were obtained using FEM element model and identified constitutive parameters.

5. Conclusions

We have proposed methodology for identification constitutive parameters of connection and material. Constitutive model of connection contain coupled plasticity-damage in hardening and nonlinear law for softening with different mechanisms of the failure. The hardening behavior is split to the bending and the shearing, but all combinations are included. The most important conclusions can be stated as follows:

- Proposed methodology is able to identify all unknown parameters(eighteen), when these parameters were split in three phases: elasticity, hardening and softening. In every phase we use local and global measurements.
- Successful identification is conditioned with enough measurments during the experimental test and adequate loading program. In this work were presented requirements for measurments (Fig. 3) and loading program. Loading program contains cycles of loading-unloading and in hardening we need to have minimal three cycles for every cases.
- The focus of this work was positioned at the behavior of the constitutive models and choice of the objective function. In the work we showed that using loading and unloading cycles we can obtain all unknown constitutive parameters. These cycles are needed to make difference between plasticity and damage model. Both models can describe same behavior in the loading regime, and only in unloading we can see difference between them.
- All cases of identification were presented in the Section 3. For illustartion of the complete procedure, we first used academic example of inverse analysis and all results of experiments were obtained from FEM model. Then, two practical examples were shown in the Section 4, but only for partial measurements that pertain to bending of connection, as the only results found in these papers. More complete experiments to fully illustrate real procedure capacity of one model are planned as the rational sequence of this work.

Acknowledgments

This work was supported financially by a doctoral scholarship from French Ministry of Foreign Affairs and French Embassy in Bosnia and Herzegovina. This support is gratefully acknowledged.

References

Ayhan, B., Jehel, P., Brancherie, D. and Ibrahimbegovic, A. (2013), "Coupled damage-plasticity model for cyclic loading: Theoretical formulation and numerical implementation", *Eng. Struct.*, **50**, 30-42.

Bui, N.N., Ngo, M., Nikolic, M., Brancherie, D. and Ibrahimbegovic, A. (2014), "Enriched Timoshenko beam finite element for modeling bending and shear failure of reinforced concrete frames", *Comput. Struct.*, **143**, 9-18.

Dujc, J., Brank, B. and Ibrahimbegovic, A. (2010), "Multi-scale computational model for failure analysis of metal frames that includes softening and local buckling", *Comput. Method. Appl. M.*, **199**(21-22), 1371-1385.

Ibrahimbegovic, A. (2009), *Nonlinear solid mechanics: Theoretical formulations and finite element solution methods*, Springer, London.

Ibrahimbegovic, A., Gharzeddine, F. and Chorfi, L. (1998), "Classical plasticity and viscoplasticity models reformulated: theoretical basis and numerical implementation", *Int. J. Numer. Meth. Eng.*, **42**(8), 1499-1535.

Ibrahimbegovic, A., Hajdo, E. and Dolarevic, S. (2013), "Linear instability or buckling problems for mechanical and coupled thermomechanical extreme conditions", *Coupled Syst. Mech.*, **2**(4), 349-374.

Ibrahimbegovic, A., Jehel, P. and Davenne, L. (2008), "Coupled damage-plasticity constitutive model and direct stress interpolation", *Comput. Mech.*, **42**(1), 1-11.

Ibrahimbegovic, A., Knopf-Lenoir, C., Kučerova, A. and Villon, P. (2004), "Optimal design and optimal control of structures undergoing finite rotations and elastic deformations", *Int. J. Numer. Meth. Eng.*, **61**(14), 2428-2460.

Ibrahimbegovic, A. and Wilson, E. (1991), "A modified method of incompatible modes", *Commun. Appl. Numer. Method.*, **7**(3), 187-194.

Kucerova, A., Brancherie, D., Ibrahimbegovic, A., Zeman, J. and Bittnar, Z. (2009), "Novel anisotropic continuum-discrete damage model capable of representing localized failure of massive structures Part II: identification from tests under heterogeneous stress field", *Eng. Comput.*, **26**(1-2), 128 -144.

Medic, S., Dolarevic, S. and Ibrahimbegovic, A. (2013), "Beam model refinement and reduction", *Eng. Struct.*, **50**, 158-169.

Mesic, E. (2003), *"Analysis of timber frames wth localized nonlinearities*", *Facta Universitatis, Series Arch. Civil. Eng.*, 2(5), Nis.

Nikolic, M. and Ibrahimbegovic, A. (2015), "Rock mechanics model capable of representing initial heterogeneities and full set of 3D failure mechanisms", *Comput. Method. Appl. M.*, **290**, 209-227.

Shi, G., Shi, Y. and Wang, Y. (2007), "Behaviour of end-plate moment connections under earthquake loading", *Eng. Struct.*, **29**(5), 703-716.

Zienkiewicz, O.C. and Taylor, R.L. (2005), *The Finite Element Method*, vol I, II, III, Elsevier.

MATLAB and Statistics Toolbox Release (2012), The MathWorks, Inc., Natick, Massachusetts, United States.